Bragg Spectroscopy of a Bose-Einstein Condensate

J. Stenger, S. Inouye, A. P. Chikkatur, D. M. Stamper-Kurn, D. E. Pritchard, and W. Ketterle

Department of Physics and Research Laboratory of Electronics, Massachusetts Institute of Technology,
Cambridge, Massachusetts 02139

Properties of a Bose-Einstein condensate were studied by stimulated, two-photon Bragg scattering. The high momentum and energy resolution of this method allowed a spectroscopic measurement of the mean-field energy and of the intrinsic momentum uncertainty of the condensate. The coherence length of the condensate was shown to be equal to its size. Bragg spectroscopy can be used to determine the dynamic structure factor over a wide range of energy and momentum transfers. [S0031-9007(99)09356-4]

The first evidence for Bose-Einstein condensation (BEC) in dilute gases was obtained by a sudden narrowing of the velocity distribution as observed for ballistically expanding clouds of atoms [1]. Indeed, most textbooks describe Bose-Einstein condensation as occurring in momentum space [2]. However, the dominant contribution to the observed momentum distribution of the expanding condensate was the released interaction energy (mean-field energy). In this paper, we present a direct measurement of the true momentum distribution of a trapped Bose-Einstein condensate, which was significantly narrower than that observed by time of flight. Furthermore, since the size of a trapped condensate with repulsive interactions is larger than the trap ground state, the momentum distribution was also narrower than that of the trap ground state. Indeed, we show that the momentum distribution of a trapped condensate is Heisenberg-uncertainty limited by its finite size, i.e., that the coherence length of the condensate is equal to its physical size.

Subrecoil momentum resolution has been previously achieved by resolving the Doppler width of a Raman transition between different hyperfine states [3] or of a two-photon transition to a metastable excited state [4]. Here we use Bragg scattering where two momentum states of the *same* ground state are connected by a stimulated two-photon process. This process can be used to probe density fluctuations of the system and thus to measure directly the dynamic structure factor $S(\mathbf{q}, \nu)$, which is the Fourier transform of the density-density correlation function and is central to the theoretical description of many-body systems [5,6]. In contrast to measuring $S(\mathbf{q}, \nu)$ with inelastic neutron scattering as in superfluid helium [7], or using inelastic light scattering [8,9], Bragg scattering as used here is a stimulated process which greatly enhances resolution and sensitivity.

Bragg scattering of atoms from a light grating was first demonstrated in 1988 [10] and has been used to manipulate atomic samples in atom interferometers [11], in de Broglie wave frequency shifters [12], and also to couple out or manipulate a Bose-Einstein condensate [13]. Small angle Bragg scattering, called recoil-induced resonances, has been used for thermometry of laser-cooled atoms [14]. In this work we establish Bragg scattering as a spectroscopic technique to probe properties of the condensate. We refer to it as Bragg spectroscopy [15] in analogy to Raman spectroscopy which involves different *internal* states.

The absorption of N photons from one laser beam and stimulated emission into a second laser beam constitutes an Nth order Bragg scattering process. The momentum transfer $\mathbf{q}$ and energy transfer $h\nu$ are given by $|\mathbf{q}| = 2N\hbar k \sin(\vartheta/2)$ and $\nu = N\Delta\nu$, where ϑ is the angle between the two laser beams with wave vector k and frequency difference $\Delta\nu$.

For noninteracting atoms with initial momentum $\hbar \mathbf{k_i}$, the resonance is given by the Bragg condition $h\nu = q^2/2m + \hbar \mathbf{k_i} \cdot \mathbf{q}/m$, which simply reflects energy and momentum conservation for a free particle. The second term is the Doppler shift of the resonance and allows the use of Bragg resonances in a velocity-selective way [13,14].

For a weakly interacting homogeneous condensate at density n, the dispersion relation has the Bogoliubov form [2]

$$\nu = \sqrt{\nu_0^2 + 2\nu_0 nU/h}, \qquad (1)$$

where $nU = n4\pi\hbar^2 a/m$ is the chemical potential, with a and m denoting the scattering length and the mass, respectively, and $h\nu_0 = q^2/2m$. For energies $h\nu \gg nU$, as probed in this paper, the spectrum is particlelike:

$$\nu \approx \nu_0 + nU/h. \qquad (2)$$

The mean-field shift nU/h reflects the exchange term in the interatomic interactions: a particle with momentum $\mathbf{q}$ experiences *twice* the mean-field energy as a particle in the condensate [2]. We use this property to determine the condensate mean-field energy spectroscopically. This is similar to the mean-field shift due to interactions with an electronically excited state which was used to identify BEC in atomic hydrogen [4].

The inhomogeneity of a trapped condensate adds two features which broaden the resonance. First, the finite size of the condensate implies a distribution of momenta which broadens the Bragg resonance due to the Doppler sensitivity of the excitation. In the Thomas-Fermi approximation, the condensate wave function $\psi(x,y,z)$ in a harmonic trapping potential is $[\psi(x,y,z)]^2 = n_0[1 - (x/x_0)^2 - (y/y_0)^2 - (z/z_0)^2]$, where n_0 denotes the peak density. The radii of the condensate (x_0, y_0, z_0) are given by $x_0 = \sqrt{2n_0U/m(2\pi\nu_x)^2}$ (similar for y_0, z_0), where ν_i are the trapping frequencies. The distribution of momenta p_x along the x axis is given by the square of the Fourier transform of the wave function [16]

$$|\psi(p_x)|^2 \sim [J_2(p_x x_0/\hbar)/(p_x x_0/\hbar)^2]^2 \qquad (3)$$

where J_2 denotes the Bessel function of order 2. This distribution is similar to a Gaussian and has an rms width of $\Delta p_x = \sqrt{21/8}\,\hbar/x_0$. Thus, the corresponding Doppler broadening of the Bragg resonance $\Delta\nu_p = \sqrt{21/8}\,q/2\pi m x_0$ is inversely proportional to the condensate size x_0 and does not depend explicitly on the number of atoms.

Second, the Bragg resonance is also broadened and shifted by the inhomogeneous density distribution of the trapped condensate. The parabolic condensate wave function gives the (normalized) density distribution $(15n/4n_0)\sqrt{1 - n/n_0}$. The simplest model for the spectroscopic line shape $I_n(\nu)$ due to the inhomogenous density assumes that a volume element with density n

leads to a line shift nU/h [Eq. (2)]:

$$I_n(\nu) = \frac{15h(\nu - \nu_0)}{4n_0U}\sqrt{1 - \frac{h(\nu - \nu_0)}{n_0U}}. \qquad (4)$$

The effect of the inhomogeneous condensate density is thus to shift the line from the free-particle resonance ν_0 by $4n_0U/7h$ (first moment), and to broaden the resonance to an rms width of $\Delta\nu_n = \sqrt{8/147}\,n_0U/h$. In contrast to the finite-size Doppler broadening, the mean-field broadening depends only on the maximum density, but not explicitly on the size.

In our experiments, both the finite-size and mean-field broadening mechanisms had to be considered. While the exact calculation of the line shape requires detailed knowledge of the excitation wave functions, the total line shift and rms width can be calculated using sum rules and Fermi's Golden Rule. Thus, it can rigorously be shown that the total line shift remains $4n_0U/7h$, while the rms width of the resonance becomes $\Delta\nu = \sqrt{\Delta\nu_p^2 + \Delta\nu_n^2}$ which is the quadrature sum of the Doppler and mean-field widths [17].

We produced magnetically trapped, cigar-shaped Bose-Einstein condensates as in previous work [18]. In order to study the resonance as a function of density and size, we prepared condensates using two different sets of trapping frequencies and varied the number of atoms by removing a variable fraction using the rf output coupler [19]. The density of the condensate was determined from the expansion of the cloud in time of flight and the size from the atom number and the trapping frequencies [18]. Bragg scattering was performed by using two counterpropagating beams aligned perpendicularly to the weak axis of the trap. Spectra were taken by pulsing on the light shortly before switching off the trap and determining the number of scattered atoms as a function of the frequency difference between the two Bragg beams. Since the kinetic energy of the scattered atoms was much larger than the mean-field energy, they were well separated from the unscattered cloud after a typical ballistic expansion time of 20 ms. Center frequencies and widths were determined from Gaussian fits to the spectra.

The duration, intensity, and detuning of the Bragg pulses were chosen carefully. The instrumental resolution is limited by the pulse duration δt_{pulse} due to its Fourier spectrum, in our case requiring $\delta t_{\text{pulse}} > 250\ \mu$s for sub-kHz resolution. The maximum pulse duration of $500\ \mu$s was chosen to be less than one quarter of the trap period by which time the initially scattered atoms would come to rest and thus would be indistinguishable from the unscattered atoms in time of flight. The light intensity was adjusted to set the peak excitation efficiency to about 20%. Sufficient detuning was necessary to avoid heating of the sample. The ratio of the two-photon rate $\omega_R^2/4\Delta$ to the spontaneous scattering rate $\omega_R^2\Gamma/2\Delta^2$ is $\Gamma/2\Delta$, where ω_R denotes the single beam

Rabi frequency, Δ the detuning, and Γ the natural linewidth. Spontaneous scattering was negligible for the chosen detuning of 1.77 GHz below the $3S_{1/2}\ F = 1 \rightarrow 3P_{3/2}\ F = 2$ transition.

The relative detuning of the two Bragg beams was realized in two ways. In one scheme, a beam was split and sent through two independent acousto-optical modulators driven with the appropriate difference frequency, and then overlapped in a counterpropagating configuration. Alternatively, a single beam was modulated with two frequencies separated by the relative detuning and backreflected. Both methods were insensitive to frequency drifts of the laser since the Bragg process only depends on the relative frequency of the two beams, which was controlled by rf synthesizers. The second method simultaneously scattered atoms in the $+x$ and $-x$ directions and was thus helpful to identify center-of-mass motion of the cloud. We estimate that residual vibrational noise broadened the line by less than 1 kHz. This resolution corresponds to a velocity resolution of 0.3 mm/s or 1% of the single-photon recoil. At a radial trapping frequency of 200 Hz, this required that the trapped condensate vibrate with an amplitude less than 0.2 μm.

Figure 1 shows typical spectra, taken both for a trapped condensate and after 3 ms time of flight when the mean-field energy was fully converted into kinetic energy. The rms width of the resonance for the ballistically expanding cloud is 20 kHz, which is much narrower than the 65 kHz wide distribution of a thermal cloud at 1 μK, a typical value for the BEC transition temperature under our conditions. We could not measure the thermal distribution with the same pulse duration as for the condensate since the fraction of scattered atoms was too small due to the broad resonance. The spectra for the thermal cloud and the expanding condensate correspond to the spatial distributions observed by absorption imaging after sufficiently long time of flight. With this technique, the BEC transition is indicated by a sudden narrowing of the time-of-flight distribution by a factor of 3. Using Bragg spectroscopy, the signature of BEC is much more dramatic—the condensate resonance is more than 30 times narrower than of the thermal cloud, and indeed narrower than that of the ground state of the trap.

Figure 2 traces the broadening of the Bragg resonance from about 2 to 20 kHz (rms width) after releasing a condensate from the trap as the mean-field interaction energy is converted into kinetic energy. After 3 ms, the momentum distribution of the cloud reached its asymptotic velocity width and expanded ballistically thereafter. Castin and Dum [20] considered the expansion of a cigar-shaped condensate in the Thomas-Fermi approximation and found that the velocity distribution should be parabolic with a maximum velocity v_x which grows as $v_x = v_\infty 2\pi\nu_x t/\sqrt{1 + (2\pi\nu_x t)^2}$, where $v_\infty = 2\pi\nu_x x_0$. To compare with our data, we combined in quadrature the Doppler width predicted by this velocity distribution, the mean-field width, and the finite-size width (assuming the size of the condensate grows as $x(t) = x_0\sqrt{1 + (2\pi\nu_x t)^2}$ [20]). As shown in Fig. 2, the agreement with our measurement is excellent.

The narrow resonance of the trapped condensate (Fig. 1) was studied as a function of the condensate density and size. Figure 3a demonstrates the linear dependence of the frequency shift on the density. The slope of the linear fit corresponds to $(0.54 \pm 0.07)n_0 U/h$, in agreement with the prediction of $4n_0 U/7h$. In Fig. 3b, the expected widths due to the mean-field energy and finite size are shown for the two different trapping frequencies studied. The data agree well with the solid lines, which represent the quadrature sum of the two contributions. To demonstrate the finite-size effect the same data are shown in Fig. 3c after subtracting the mean-field broadening and the finite pulse-length broadening (0.5 kHz). The linewidths are consistent with the expected $1/x_0$ dependence. Even without these corrections the measured linewidths are within 20% of the value expected due to the Heisenberg-uncertainty limited momentum distribution (Fig. 3b).
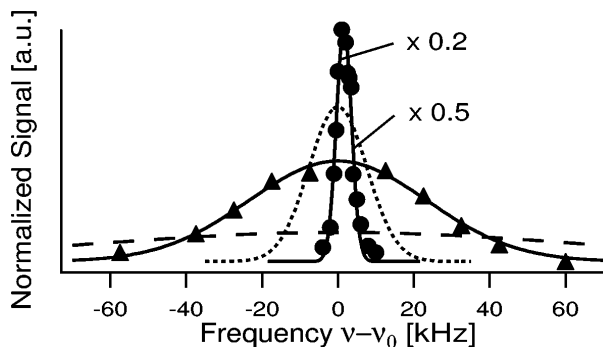

FIG. 1. Bragg resonances for a trapped condensate (circles) and after 3 ms time of flight (triangles). For comparison, the momentum distributions of the ground state of the trapping potential (dotted curve) and of a 1 μK cold, thermal cloud (dashed curve) are indicated. The heights of the curves for the trapped condensate and the ground state momentum distribution are scaled down as indicated in the figure.
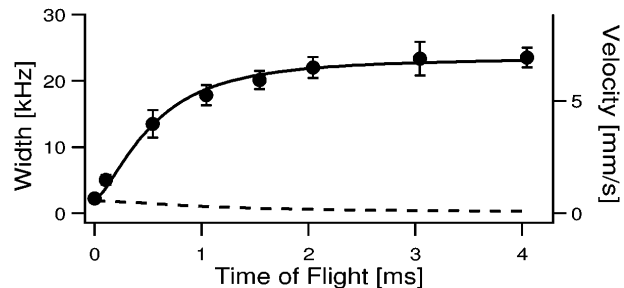

FIG. 2. Mean-field acceleration of a condensate released from the trap. Shown is the increase of the rms width of the Bragg resonance during the expansion. The solid line is the theoretical prediction [20] using the trap frequency $\nu_x = 195$ Hz. The dashed line represents the contributions of mean-field energy and finite size to the total width.
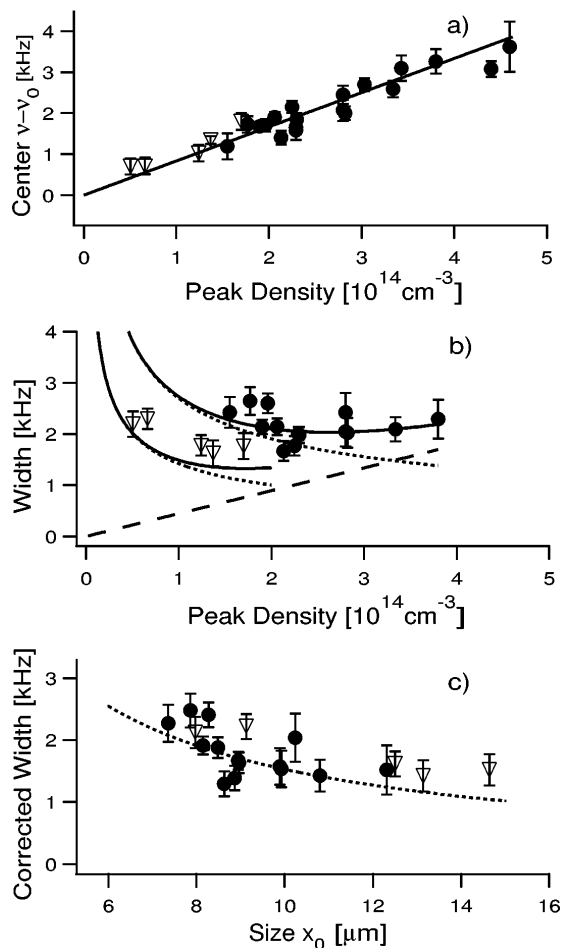
FIG. 3. Bragg spectroscopy of a trapped condensate. Line shifts (a) and rms widths (b) are shown for various densities and sizes of the condensate using two different radial trapping frequencies, $\nu_x = (195 \pm 20)$ Hz (circles), and $\nu_x = (95 \pm 20)$ Hz (triangles). The lines in (b) show the contributions of the mean-field energy (dashed) and due to the finite size (dotted, for both trapping frequencies) and their quadrature sum (solid lines). (c) displays the width after subtraction of the contribution of the mean field and the finite pulse duration and compares it with the prediction for the momentum uncertainty due to the finite size. The error bars are 1σ errors of the Gaussian fits to the data.

The momentum spread of the condensate is limited by its coherence length x_c which, in the case of long-range order, should be equal to the size x_0 of the condensate. Our results show that $x_c \approx x_0$ in the radial direction of the trap, thus providing a quantitative measure of the long-range coherence observed earlier by interfering two condensates [21]. In particular, our measurements indicate that the condensate does not have phase fluctuations on this length scale, i.e., that it does not consist of smaller quasicondensates with random relative phases. It would be interesting to measure the coherence length during the formation of the condensate, e.g., after suddenly quenching the system below the BEC transition

temperature [22], and to observe the disappearance of phase fluctuations.

In this work we have energy resolved the response of the condensate to a momentum transfer of two photon recoils, constituting a measurement of the dynamic structure factor $S(\mathbf{q}, \nu)$ for this value of $\mathbf{q}$. Different momentum transfers are possible by changing the angle between the Bragg beams and/or the order N of the Bragg transition, thus enabling measurements of $S(\mathbf{q}, \nu)$ over a wide range of parameters. At low momentum transfer, the line shape is dominated by the mean-field energy and by phononlike collective excitations, whereas at high momentum transfers, the linewidth mainly reflects the momentum distribution of individual atoms. This is analogous to neutron scattering in liquid helium, where slow neutrons were used to observe the phonon and roton part of the dispersion curve, and fast neutrons were used to determine the zero-momentum peak of the condensate [7]. While we have observed higher-order Bragg scattering up to third order in the trapped condensate using higher laser intensities, its spectroscopic use was precluded by severe Rayleigh scattering, and would require larger detuning from the atomic resonance.

The use of inelastic light scattering to determine the structure factor of a Bose-Einstein condensate was discussed in several theoretical papers [8,9]. It would require the analysis of scattered light with kHz resolution and suffers from a strong background of coherently scattered light [9]. Bragg spectroscopy has distinct advantages because it is a stimulated, background-free process in which the momentum transfer and energy are predetermined by the laser beams rather than postdetermined from measurements of the momentum and energy of the scattered particle.

In conclusion, we have established Bragg spectroscopy as a new tool to measure properties of a condensate with spectroscopic precision. We have demonstrated its capability to perform high-resolution velocimetry by resolving the narrow momentum distribution of a trapped condensate and by observing the acceleration phase in ballistic expansion. Since the momentum transfer can be adjusted over a wide range, Bragg spectroscopy can be used to probe such diverse properties as collective excitations, mean-field energies, coherence properties, vortices, and persistent currents.

[1] M. H. Anderson *et al.*, Science **269**, 198 (1995); K. B. Davis *et al.*, Phys. Rev. Lett. **75**, 3969 (1995).

[2] K. Huang, *Statistical Mechanics* (Wiley, New York, 1987), 2nd ed.

[3] M. Kasevich *et al.,* Phys. Rev. Lett. **66**, 2297 (1991).

[4] D. G. Fried *et al.,* Phys. Rev. Lett. **81**, 3811 (1998); T. C. Killian *et al., ibid.* **81**, 3807 (1998).

[5] T. J. Greytak, in *Quantum Liquids,* edited by J. Ruvalds and T. Regge (North-Holland, New York, 1978).

[6] A. Griffin, *Excitations in a Bose-Condensed Liquid* (Cambridge University Press, Cambridge, 1993).

[7] P. Sokol, in *Bose-Einstein Condensation,* edited by A. Griffin, D. W. Snoke, and S. Stringari (Cambridge University Press, Cambridge, 1995); P. Nozieres and D. Pines, *The Theory of Quantum Liquids* (Addison-Wesley, Reading, 1994).

[8] J. Javanainen, Phys. Rev. Lett. **75**, 1927 (1995); R. Graham and D. Walls, Phys. Rev. Lett. **76**, 1774 (1996); A. S. Parkins and D. F. Walls, Phys. Rep. **303**, 1 (1998), and references therein.

[9] H. D. Politzer, Phys. Rev. A **55**, 1140 (1996).

[10] P. J. Martin, B. G. Oldaker, A. H. Miklich, and D. E. Pritchard, Phys. Rev. Lett. **60**, 515 (1988).

[11] D. M. Giltner, R. W. McGowan, and S. A. Lee, Phys. Rev. Lett. **75**, 2638 (1995).

[12] S. Bernet *et al.,* Phys. Rev. Lett. **77**, 5160 (1996).

[13] M. Kozuma *et al.,* Phys. Rev. Lett. **82**, 871 (1999).

[14] J.-Y. Courtois, G. Grynberg, B. Lounis, and P. Verkerk, Phys. Rev. Lett. **72**, 3017 (1994).

[15] P. R. Berman and B. Bian, Phys. Rev. A **55**, 4382 (1997).

[16] G. Baym and C. J. Pethick, Phys. Rev. Lett. **76**, 6 (1996).

[17] D. M. Stamper-Kurn (to be published).

[18] M.-O. Mewes *et al.,* Phys. Rev. Lett. **77**, 416 (1996).

[19] M.-O. Mewes *et al.,* Phys. Rev. Lett. **78**, 582 (1997).

[20] Y. Castin and R. Dum, Phys. Rev. Lett. **77**, 5315 (1996).

[21] M. R. Andrews *et al.,* Science **275**, 637 (1997).

[22] H.-J. Miesner *et al.,* Science **279**, 1005 (1998); D. M. Stamper-Kurn *et al.,* Phys. Rev. Lett. **81**, 2194 (1998).